Cellular automata approach for morphological evolution of localised corrosion

Dung Di Caprio, Christine Vautrin-Ul, J. Stafiej, A. Chaussé, D. Féron, J Badiali

Cellular automata approach for morphological evolution of localised corrosion.

D. Di Caprio[1], C. Vautrin-Ul*[2], J. Stafiej[3], A. Chaussé[2], D. Féron[4], J.P. Badiali[1]

[1] *Laboratoire d'Electrochimie, Chimie des Interfaces et Modélisation pour l'Energie, Chimie Paris Tech, ENSCP, CNRS, 4 place Jussieu, 75005 Paris, France*
[2] *Laboratoire Analyse et Modélisation pour la Biologie et l'Environnement, UMR 8587, CNRS-CEA-Université d'Evry Val d'Essonne, Bd F. Mitterrand 91 025 Evry, France*
[3] *Institute of Physical Chemistry, Polish Academy of Sciences, ul. Kasprzaka 44/52, 01-224 Warsaw, Poland*
[4] *Service de la Corrosion et du comportement des Matériaux dans leur Environnement, CEA, DEN, Bâtiment 458, 91 191 Gif sur Yvette Cedex, France*

Abstract

We present a cellular automata approach to the morphology evolution of a corroding metal surface. In the model, we consider a morphology dependent corrosion probability of a site on the corrosion front. Selecting the model parameters we are able to reproduce a variety of different pit shapes and morphological regimes ranging from narrow pore like channels to broader cavities. In the model, we control the ratio between localised and uniform corrosion. A diffusion process is also taken into account. The model is capable of predicting different scenarios for the evolution of the corrosion front in time.

Keywords

Cellular automata ; Pitting Corrosion ; Diffusion ; Morphology

1. Introduction

In a recent article[1], we present a simple model of localised corrosion and show how within a unified framework it can predict different morphologies for the corrosion front. Understanding the underlying mechanisms of localised corrosion and the competition with the uniform corrosion is an important issue. Indeed, although localised corrosion is limited in space, it generally has a rapid kinetic rate and by forming cavities or pits it is sufficient to damage most devices. In our model we distinguish two regions of the metal surface where the corrosion takes place corresponding to localised and uniform corrosion. The origin of surface heterogeneities can be of

different nature: mechanical (inclusions, grain boundaries, dislocations ...) or chemical such as different chemical composition inside pits or cavities due to the time necessary to evacuate the reaction products[2-6]. These heterogeneities are random in time and space. This is the reason why our description is based on a cellular automata (CA) model. Such models have proved powerful tools in the study of interfaces e.g. metal-electrolyte interfaces[7-14]. They have the advantage of remaining simple and still be versatile. We introduce essentially two parameters λ , ε which define two regions and their respective corrosion rates. Another parameter ϕ is related to the Pilling Bedworth[15] (PB) parameter and modifies the molar volume of the oxide with respect to that of the metal. In our previous paper, the value of ϕ was 1. In this event, the localised corrosion takes place with a reaction rate constant throughout the simulation. Here, we study the case $\phi = 2$ when the specific oxide volume is much larger than that of equivalent metal. The products of reaction take up more space and due to steric exclusion the reaction product needs to diffuse away from the corroded metal interface, before the corrosion process can continue. Therefore there is a coupling between corrosion and diffusion and this mechanism can modify the effective corrosion rate throughout corrosion. The aim of this paper is to study the evolution in time of the corroded surface in relation with its morphological features. For the long term prediction of the corrosion behaviour of alloys used in nuclear waste disposal, it is important to know the morphological evolution of corroded surfaces and in particular if localised corrosion will stop. Experimental and field data indicate that the importance of localised corrosion decreases over time. This is traditionally characterized by a vanishing pitting factor in time[16]. This work is the first development to investigate whether cellular automata can help understanding the evolution of the pitting factor.

The paper is organised as follows, Section 1 presents the model. In Section 2, examples of morphologies obtained by varying the spatial and kinetic parameters and setting the parameter $\phi = 1$ are shown. In Section 3, we discuss the time dependence of the corrosion giving results for

values of $\phi = 1$ and 2 and compare the morphology evolution for them. Some conclusions and perspectives are given at the end.

2. Electrochemical and CA models

We first give a brief description of the corrosion model and its transcription into CA formalism, the reader is referred to [1] for a detailed description of the model. In terms of CA, we have (Fig.1): metal sites (*M*), reactive metal (*R*) which is a metal site adjacent to a solution which can be a solution site (*S*) or within a porous layer site (*L*) and diffusive sites (*D*).

We have shown that the film formation on a metal can be described in terms of three main processes[1] (Fig.1):

- two chemical reactions one at the corrosion front (1) and one at the film-solution interface (2)
- diffusion process of the intermediate corrosion products across the layer already formed.

The porous layer formed can be seen at the mesoscopic scale as an interconnected lattice and allows for the contact of the metal with the aggressive solution thus maintaining the corrosion process alive. The diffusing (*D*) sites are introduced to account for the stoichiometric balance of the metal together with the well known fact that the specific volume of the oxide is larger than that of the original metal. This is known as the PB parameter which is related to ϕ. For one corroded metal site, ϕ sites (*D*) are created. Therefore corrosion can always take place when $\phi = 1$, as the diffusing metal can accommodate in the porous layer site which replaces the metal. When $\phi = 2$, the corrosion proceeds only if there is sufficient place in the neighbourhood of the corroded site to accommodate the larger volume excess of diffusing metal. In terms of our model this is possible when at least one nearest neighbours is an (*S*) or (*L*) site. The existence of these free sites

is related to the ability of previously created (*D*) sites to diffuse away from the corrosion front. We will see that a slow diffusion of (*D*) sites can drastically slow down the corrosion rate.

The probability of transformation of a metal (*R*) site is *p*'. It is a function of an intrinsic corrosion rate parameter *p* and two local parameters λ and ε. *p* depends on the properties of the aggressive solution but does not evolve with the oxide layer formation. There are two characteristic times: one for corrosion, one for diffusion. They are identical when *p*=1, which we suppose first. Assuming the simulation site is a cube of 10 nm side, we obtain, for a 1mm/year corrosion rate, that one metal site is corroded in roughly 5 minutes. The estimation is purely indicative as corrosion rates are extremely different according to metal and environmental conditions. However, such time scale is large in comparison to atomic scale simulations and short with respect to time scales for corrosion which justifies our mesoscopic CA stochastic models. For p=1, the typical diffusion coefficient is between 10^{-13} and 10^{-15} m^2/s depending on the properties of the porous layer. Such a coefficient is low compared to ordinary bulk diffusion in liquid, however we have a porous structure. Also for smaller *p*, for identical corrosion rate, we decrease the corrosion probability and thus the time step. In parallel, the diffusion coefficient is multiplied by 1/*p* and for the values of *p* presented we obtain typical values of the diffusion coefficient. The parameter λ defines the extension of two regions in the pit where reactivity is different and ε modulates the probability in them (Fig.2). The probability of corrosion is finally given by *p*' which is *p* modulated by λ and ε. Physically, λ and ε introduce the morphology dependent metal reactivity in relation to environment, faster corrosion at the bottom of cavities, pits. When $\phi \geq 2$, there is another modulation of the probability due to the local environment, a free site able to accommodate the diffusing metal must exist. The corrosion events now depend on the specific evolution of a corrosion front.

3. Comparison with experimental morphologies.

The model introduced above is a simple model to mimic uniform and localised corrosion. In terms of electrochemical reactions, we assume that the anodic reaction (oxidation of metal) occurs preferentially at the bottom of the pit, and is less active near the top or on the surface outside the pit. In these regions (top and outside the pit) the cathodic reaction occurs preferentially. We study the cases ϕ=1 and ϕ=2. In the first instance one metal site produces two (L) sites. These sites are porous entities. For instance, we can consider that 2/3 of their volume is filled with the product leaving 1/3 for the pores. Such value corresponds to a site filled by oxide but leaving enough space for solution to flow across. Having produced two (L) sites the PB parameter is 2*2/3=1.33 close to typical values for Al or Pb[15]. Whereas the case ϕ=2 corresponds to the creation of three (L) sites. Considering an identical filling ratio of 2/3, we now have that the corresponding PB parameter is 2. This is close to values observed for Fe, Cr[15]. This correspondence is clearly approximate as we have only estimate a filling ratio for the (L) sites and cannot deal with fractions of sites.

3.1. Examples of morphologies for ϕ =1.

Hereafter is an example of cracks observed in carbon steel and their simulation equivalent obtained for ϕ = 1, p = 0.005, λ = 0.999 and the values of ε are indicated on each snapshot in Fig.3. λ close to 1 corresponds to a preferential corrosion at the bottom of pits and vanishing ε to a much faster corrosion rate also at the bottom. We observe that varying ε from 0.001 to 0.1 morphologies change gradually from narrow to larger cracks. This influence of ε suggests that large cracks can correspond to conditions where uniform corrosion is higher. Note that the three snapshots are obtained for identical number of simulation time steps, therefore for ϕ = 1, there is no direct relation between the geometry and the time evolution. One can also check that the overall probability p does not have any other effect than modifying the overall time scale, events are more

or less rapid. Applying identically to both regions of different kinetics, the morphologies are not modified. The cracks observed on carbon steel (Fig.3) have been obtained under identical conditions. Being more or less opened is attributed to local stress conditions. The results obtained with CA modelling show that the local conditions (distribution of anodic and cathodic reactions for instance or local stress) might explain the fact that cracks are more or less open.

In Fig.4, we show other examples of cracks obtained in different conditions, where we have an illustration that the process is fundamentally stochastic with a geometry which cannot be determined in advance. The CA simulations mimic rather well such property.

3.2. Morphologies in the case ϕ=2.

In this Section, we study the case $\phi = 2$. We choose to present, in Fig.5, snapshots for identical values of λ and ε but different values of *p,* parameter with no effect on the morphology when ϕ=1.

For identical λ and ε, morphologies now depend on *p*. Dynamic aspects will be discussed in detail in Section 3.3. However, we can compare for $p = 0.005$ simulation times corresponding to the same pit depth for the $\phi = 1$ and 2. The two values respectively 47300 and 1335000 time steps are quite different. Typically for $\phi = 2$, the simulation time is higher owing to a slow down due to the diffusion process. We observe that the morphologies become more open towards the surface when *p* increases. This can be understood as follows. The higher *p*, the greater the corrosion rate and therefore the number of diffusing (*D*) sites produced. These sites have to diffuse from the metal interface before new metal sites can be corroded. The localised corrosion rate which is originally much higher at the bottom of the pit for $\varepsilon = 0.001$ gradually slows down therefore reducing effectively the difference in value of the kinetics between the upper and lower regions. Such behaviour has been observed for ϕ=1 in Fig.5 and [1], when ε increases.

3.3. Time evolution.

Varying the parameter *p,* in the case ϕ=2, does not only have an effect on the morphology but also affects the evolution in time of the pit depth. These predictions can be interesting for comparison with experimental data in order to distinguish different models and mechanisms, as the evolution of the pit depth can be measured. The growth of pits are known to have a power dependence with time[9,17-19]. In the following we compare for λ = 0.99 and ε = 0.001, Log(h_b) the logarithm of the depth of the pit (pit depth + general corrosion thickness), see Figure 2 as a function of Log(T) (logarithm of the simulation time), for ϕ = 1 and 2.

3.3.1 Time evolution of the pit for ϕ = 1.

In Fig.6, we present the case ϕ = 1, for five values of p. Although morphologies do not depend on p, the evolution in time does. The dependence of Log(h_b) with Log(T) corresponds roughly to straight lines with expected slope of one. This value is not too accurate for small values p, as the number of events diminishes leading to a poor statistics. However, for the more accurate case when p = 0.5, we obtain a value of the slope of 1.04. The value is not as close to 1 as in Saunier *et al.*[9] because here we consider the evolution of a single pit compared to the statistical average evolution of a whole front and iterated simulations which are unfortunately time consuming. Note also, that linear fits are from the last part of the curves. The beginning is not relevant as from the flat front we have a transient regime before the growing pit regime is well established. Another consequence of the existence of a transient regime is that the constant in the linear fits cannot be directly related to Log(p). Nonetheless, we can verify that for a given value of Log(h_b) for instance 7, two successive lines are separated in terms of Log(T) by a value close to 2.3 ± 0.03 which corresponds to decreasing p by a factor 10.

Concerning corrosion phenomena and surface evolution, the linear relationship between Log(h_b) and Log(T) implies a constant corrosion rate while it is generally observed, particularly under

repository conditions with carbon steel, that the corrosion rate decreases in time, especially at the beginning of exposure due to the formation of the oxide layer. So other conditions need to be modelled: this is why we introduce diffusion processes with $\phi = 2$.

3.3.2 Time evolution of the pit for $\phi = 2$.

When $\phi = 2$, we observe that the time dependence is not always linear as for $\phi = 1$. In Fig.7, for $p = 0.5$, the curve is close to linear, the slope 0.49 is close to 0.5 characteristic of diffusion. Indeed, the corrosion process is controlled by the diffusion of (D) sites[9-10] which have to leave the metal interface before a new corrosion process takes place. For other p, we observe that the slope varies in time. In Figure 5, for an identical height the number of simulation time steps do not follow a simple proportionality law with p as for $\phi = 1$. As a consequence the distance between curves for a given value of Log(h_b) cannot be analysed as it now varies in time. This is a sign that we have different regimes in the course of the evolution. For instance for $p = 0.005$, the slope is around 0.5 at the beginning of the simulation, it decreases reaching 0.3 and finally reaches 0.54. Such a phenomenon can be understood for instance observing the snapshot for $p = 0.005$, in Figure 5. We can observe a narrow part in the pit which behaves as a bottle neck for the diffusion of (D) sites out from the cavity. The slow down in the kinetic rate is associated to the formation of this bottle neck. Its configuration is capable of slowing down the diffusion which explains the values of the slope below 0.5. In the cases $p = 0.0005$ and $p = 0.00005$, we observe that the power law initially has an exponent which is larger than 0.5. For intermediate values of time we have slopes of 0.66 and 1.2 respectively which gradually fall to 0.5 and 0.48. Thus at the beginning of the simulation the production of (D) sites is small and there is sufficient time for a (D) site to diffuse before the following site is created. Then the pit gets deeper and widens at the bottom, the number of sites which can produce (D) sites, increases. Due to the crowding of (D) sites and to a longer pit, we fall into the diffusion limited regime. The results obtained for ϕ=2 are more representative for the

experimental observations where the power law exponent can have values from 0.05 and 0.5 and more commonly between 0.3 and 0.5[18]. When the exponent is 0.5 the process is thought to be governed by ohmic or diffusion controlled phenomena[17-19]. In this study, we observes that in all cases the exponents tend toward the 0.5 value for long time simulations. In the intermediate regimes, we observe transient behaviours where the exponent can have different values due to the evolution of the morphology. These values lie in the range of the experimental values.

4. Concluding remarks

In this paper, we discuss new aspects of a simple model of localised corrosion. In a previous paper, we have shown that this simple model can describe a variety of different morphologies and emphasized the interest of our stochastic CA approach. In particular, within this approach we do not select a priori the location and geometry of localised corrosion as generally the case within continuous models. We focus on the influence of a diffusion process on the evolution of the corrosion front. Two cases are compared one where diffusion does not have any effect on the corrosion rate ($\phi = 1$), one where the diffusion of species between the corrosion front ant the oxide-solution interface plays a role ($\phi = 2$). In this study we learn that owing to the existence of another time scale related to diffusion, there is a correlation between diffusion and the velocity of the corrosion process. Typically, we find that the diffusion slows down corrosion and produces a new effective kinetic rate of corrosion different than the one initially set by the parameters. This effective kinetic rate can be compared to the results for $\phi = 1$ and a suitable value of the parameter ε. The evolution of the morphology is then dependent on this effective corrosion and in turn can again modify the kinetic rate. The systems goes through different regimes with strong or week diffusion limitation and slow or fast corrosion rates.

This work is essentially a first step in the investigation of the time dependence of corrosion emphasizing the existence of correlations between the morphology and the evolution in time. In

this study, we characterize pits by their overall depth defined from the initial position of the metal interface. Whereas experiments generally measure the final morphology of the corroded metal and the pit depth also accounts for the uniform corrosion contribution. In the future, we intend to complete this study by taking this into account as well as the pH[18] in relation to passivation. This effect can have consequences on surface properties of the metal, porosity of the oxide layer and diffusion across this layer. The various properties can be adapted in our simulation model to describe experimental situations. This will help understanding and predicting the evolution of quantities such as the pitting factor for long term predictions where direct observation are difficult.

References.

[1] Di Caprio, D., Vautrin-Ul, C., Stafiej, J., Saunier, J., Chaussé, A., Féron, D., Badiali, J.P., *Corros.Sci.* 2010, 53, 418-425.

[2] Landolt D., Corrosion et Chimie de Surfaces des Métaux, Traité de Matériaux, 12, Presses Universitaires et Polytechniques Romandes, Lausanne 1997.

[3] Corrosion Chemistry within Pits, Crevices, and Cracks, A. Turnbull, Editor, HMSO Books, London (1987).

[4] Critical Factors in Localized Corrosion, Frankel G. S. and Newman R. C., Editors, PV 92-9, The Electrochemical Society Proceedings Series, Pennington, NJ (1992).

[5] Burstein, G.T., Liu, C., Souto, R.M., Vines, S.P., *Science and Technology* 2004, 39, 25–32.

[6] Williams, D. E., Westcott, C., Fleischmann, M., *J.Electrochem.Soc.*1985,132, 1804-1811.

[7] Cordoba-Torres, P., Nogueira, R. P., Fairén, V., *Electrochim.Acta* 2002, 529, 109.

[8] Córdoba-Torres, P., Nogueira, R.P., Fairén, V., *J.Electroanal.Chem.* 2003, 560, 25.

[9] Saunier, J., Chaussé, A., Stafiej, J., Badiali, J.P., *J.Electroanal.Chem.* 2004, 563, 239.

[10] Saunier, J., Dymitrowska,M., Chaussé, A., Stafiej, J., Badiali, J.P., *J.Electroanal.Chem.* 2005, 582, 267.

[11] C. Vautrin-Ul, A. Taleb, J. Stafiej, A. Chaussé, J.P. Badiali, Electrochemica Acta, 2007, 52, 5368.

[12] Vautrin-Ul, C., Mendy,H., Taleb, A., Chaussé, A., Stafiej, J., Badiali, J.P., *Corros.Sci.* 2008, 50, 2149.

[13] Vautrin-Ul, C., Chaussé, A., Stafiej, J., Badiali, J.P., *Polish Journal of chemistry* 2004, 78, 1795.

[14] Stafiej, J., Taleb, A., Vautrin-Ul, C., Chaussé, A., Badiali, J.P., *Passivation of Metals and semiconductors, and Properties of Thin oxide Layers* P. Marcus, V. Maurice(Ed.), Elsevier, Paris, 2006, pp.667.

[15] Pilling, N., Bedworth, R., *J. Inst. Met.* 1923, 29, 529-591

[16] Santarini, G., "Prediction of long term corrosion behaviour in nuclear waste systems" Proceedings of the 2nd international workshop, Nice, France, 2004, Eurocorr2004, p.97-105.

[17] Z. Szklarska-Smialowska, Corros.Sci. 1999, 41, 1743.

[18] M.K. Cavanaugh, R.G. Buchheit, N. Birbilis, Corros.Sci. 2010, 52, 3070.

[19] K.K. Sankaran, R. Perez, K.V. Jata, Materials Science and Engineering 2001, A297, 223.

Captions

Figure 1:
Simple scheme of the forming layer with clusters and solution representation of reaction (1) and (2).

Figure 2:
Definition of λ and ε. λ defines the extension of the top region where the probability of corrosion is pε. In the remaining bottom area the probability of corrosion is p (1-ε).

Figure 3: cracks observed on carbon steel exposed to carbonated soil water(constant deformation test). Simulated pits for different values of λ and ε as indicated on the figure for identical number of time steps. The metal is shown in black, pink points are the diffusing (*D*) sites, green the passive layer (*L*) sites and grey the solvent. This colour code is used from now on.

Figure 4: (a) Intergranular cracks in alloy 600 in water circuit polluted with lead at 360°C (b) Snapshots obtained for $\lambda = 0.978$ and $\varepsilon = 0.001$.

Figure 5: Snapshot obtained for the identical values of $\lambda = 0.99$ and $\varepsilon = 0.001$, the first snapshot is for $\phi = 1$, the following ones are for $\phi = 2$ and the value of p and the number of simulation time steps T is as indicated on the figure.

Figure 6: Logarithm of h_b as a function of the logarithm of the time T for p = 0.5, 0.05, 0.005, 0.0005 and 0.00005 from left to right. The parameters are $\lambda = 0.99$ and $\varepsilon = 0.001$. The functions y are linear fits of the corresponding curves in the final part of the curves, full lines.

Figure 7: Logarithm of h_b as a function of the logarithm of the time T. The parameters are $\lambda = 0.99$ and $\varepsilon = 0.001$. The functions y and y1 are linear fits of the corresponding curves respectively full lines and points (diamonds) for the different regions.

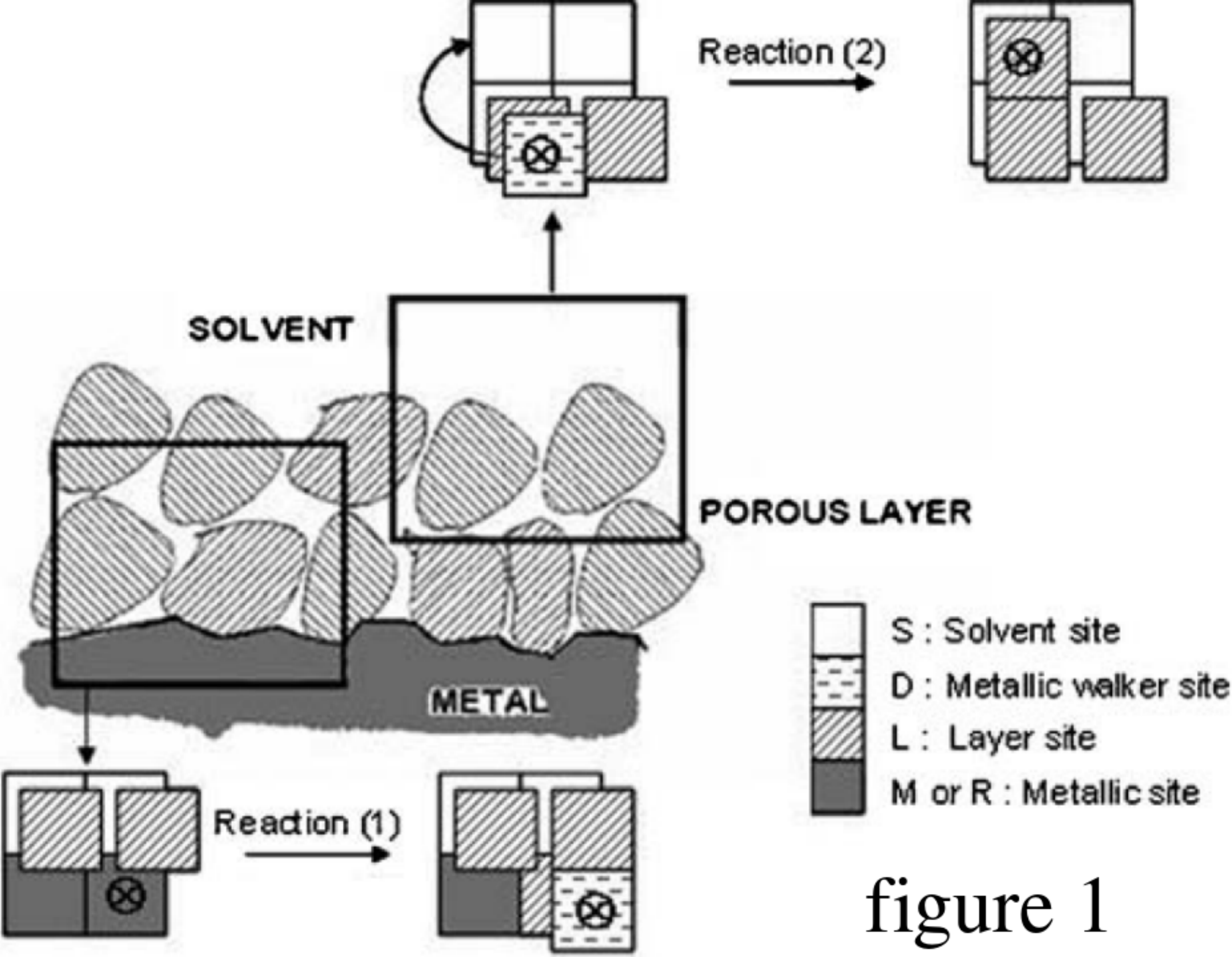
Reaction (2)
SOLVENT
POROUS LAYER
METAL
Reaction (1)
S : Solvent site
D : Metallic walker site
L : Layer site
M or R : Metallic site

figure 1

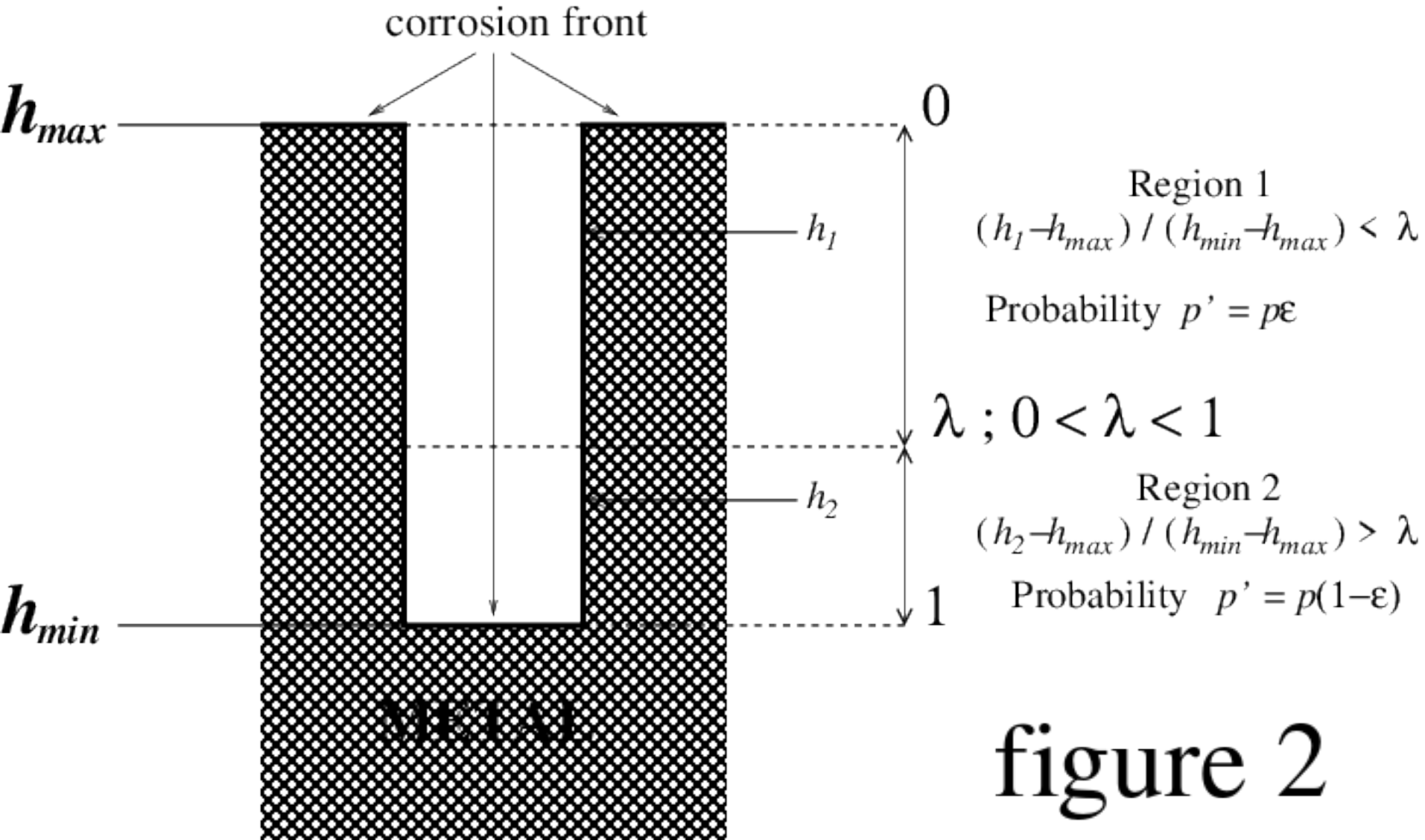
corrosion front
h_{max}
h_{min}
0
h_1
h_2
1
λ ; 0 < λ < 1
Region 1
$(h_1 - h_{max}) / (h_{min} - h_{max}) < \lambda$
Probability $p' = p\varepsilon$
Region 2
$(h_2 - h_{max}) / (h_{min} - h_{max}) > \lambda$
Probability $p' = p(1-\varepsilon)$
METAL

figure 2

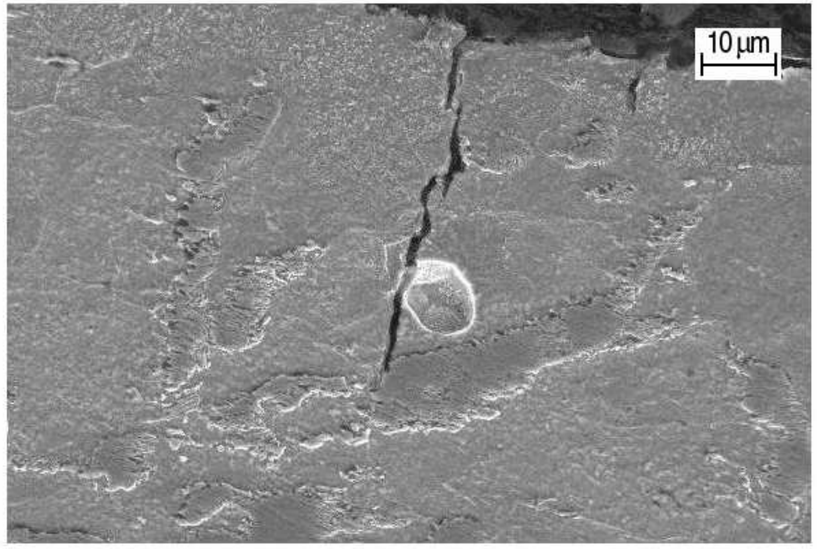

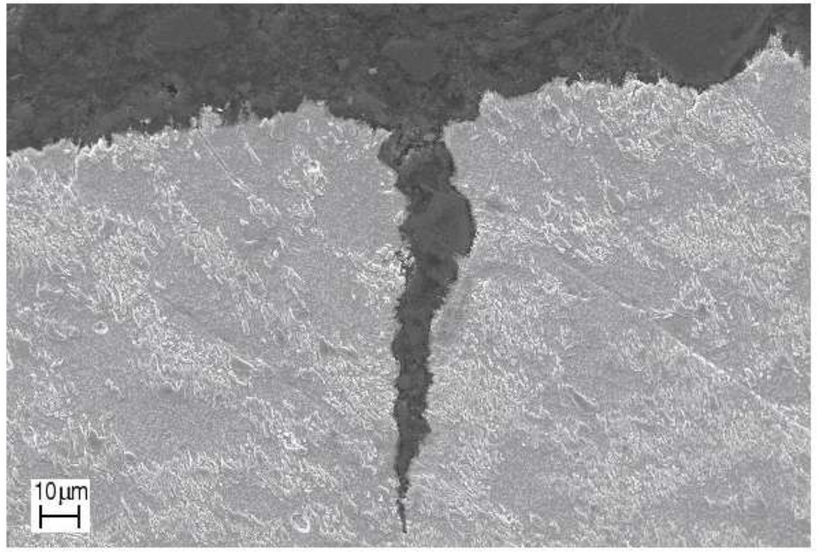

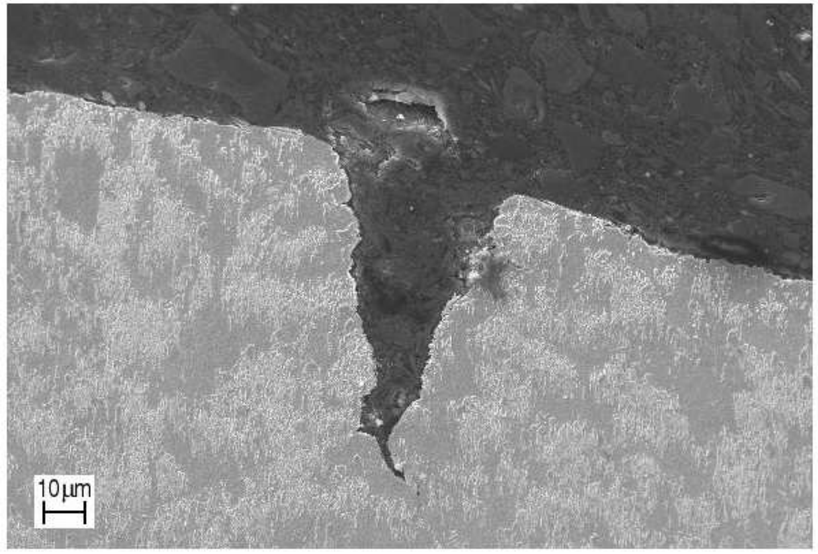

figure 3

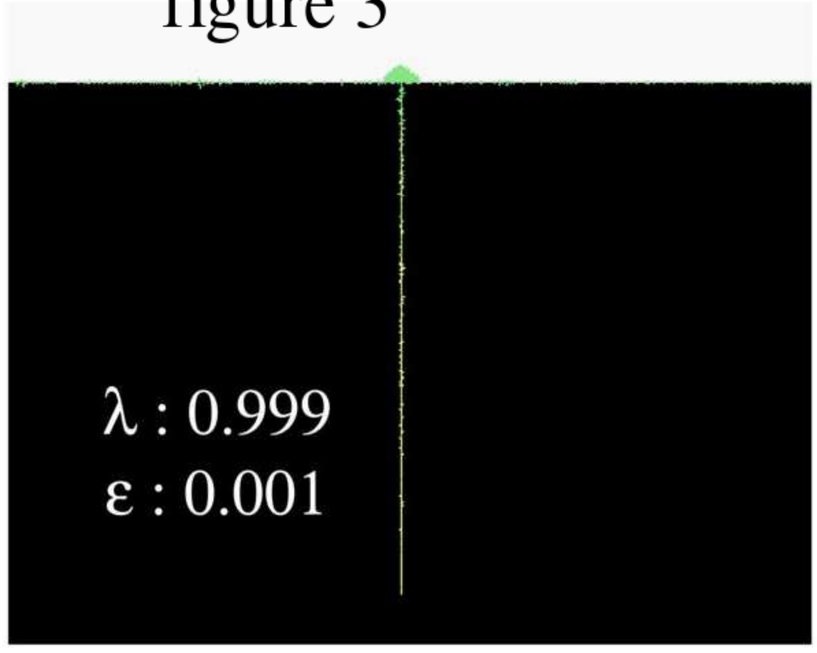

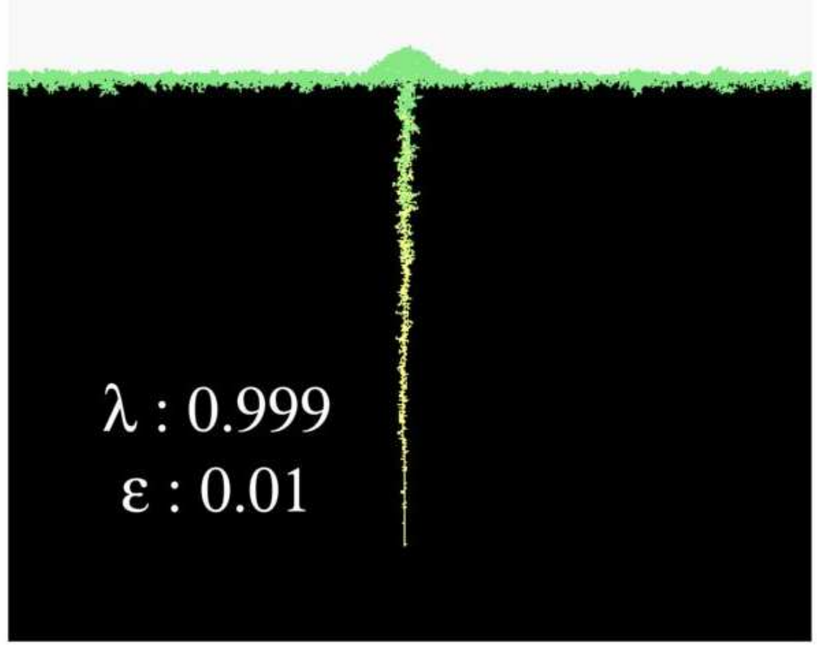

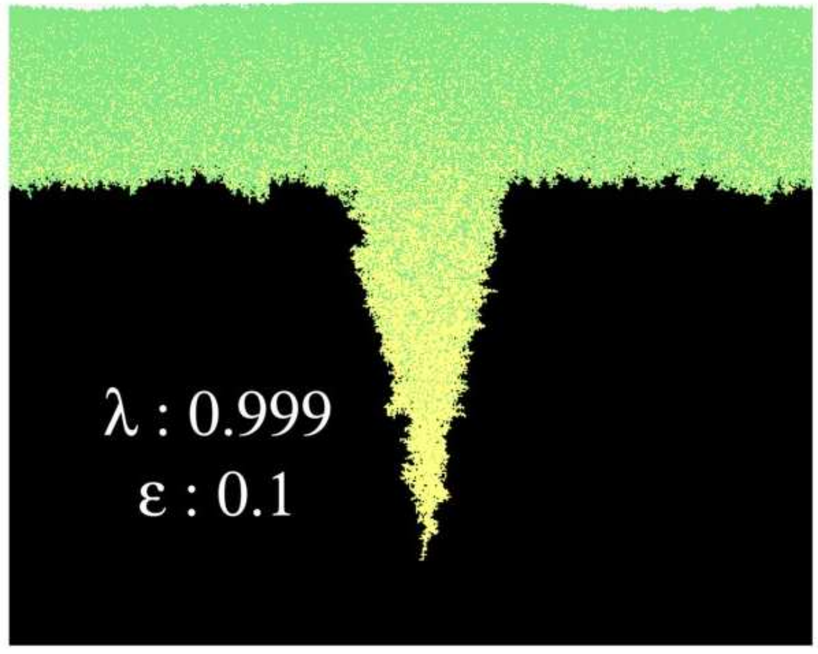

figure 4

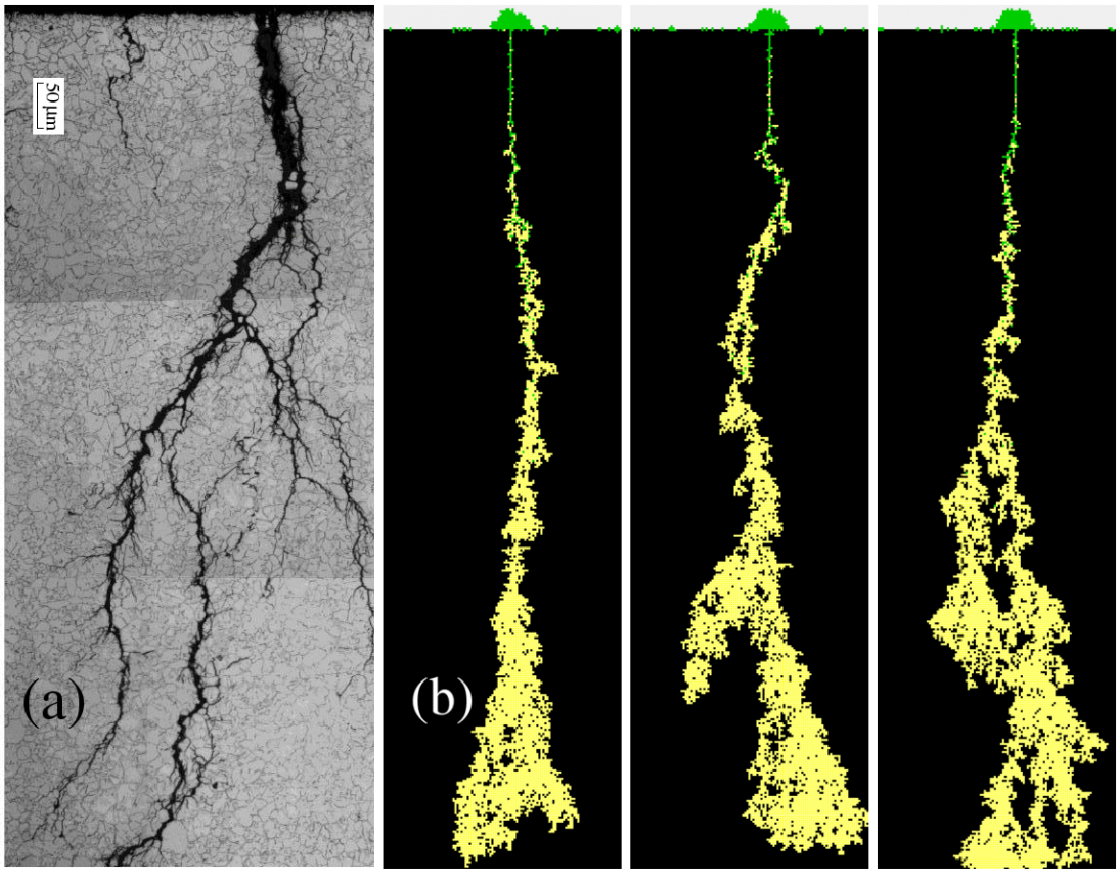

figure 5

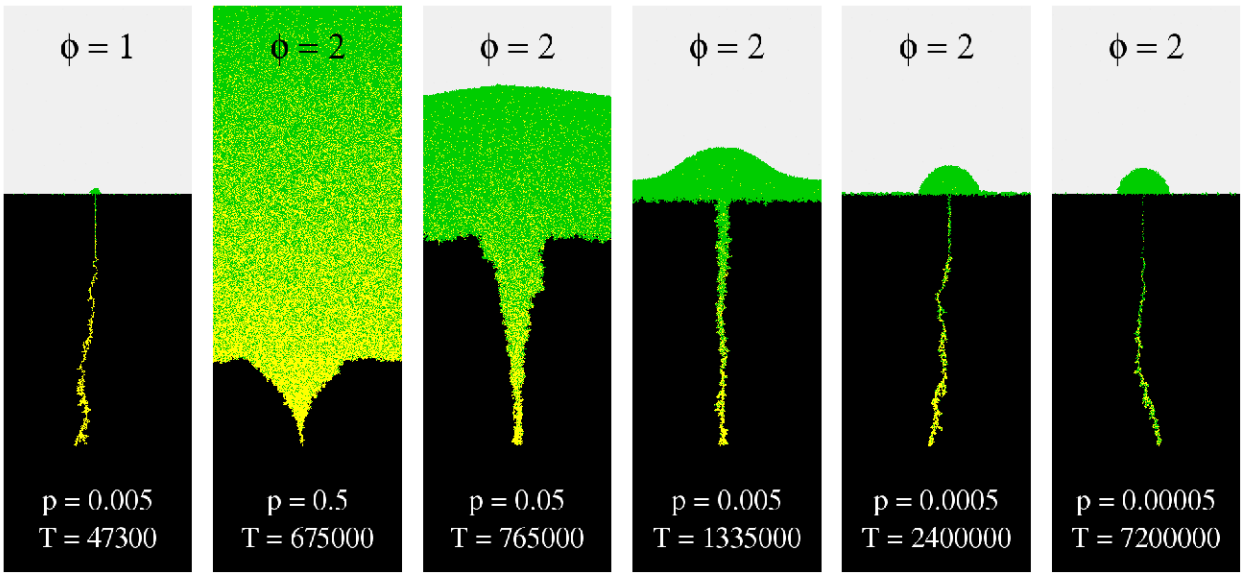
ϕ = 1
p = 0.005
T = 47300
ϕ = 2
p = 0.5
T = 675000
ϕ = 2
p = 0.05
T = 765000
ϕ = 2
p = 0.005
T = 1335000
ϕ = 2
p = 0.0005
T = 2400000
ϕ = 2
p = 0.00005
T = 7200000

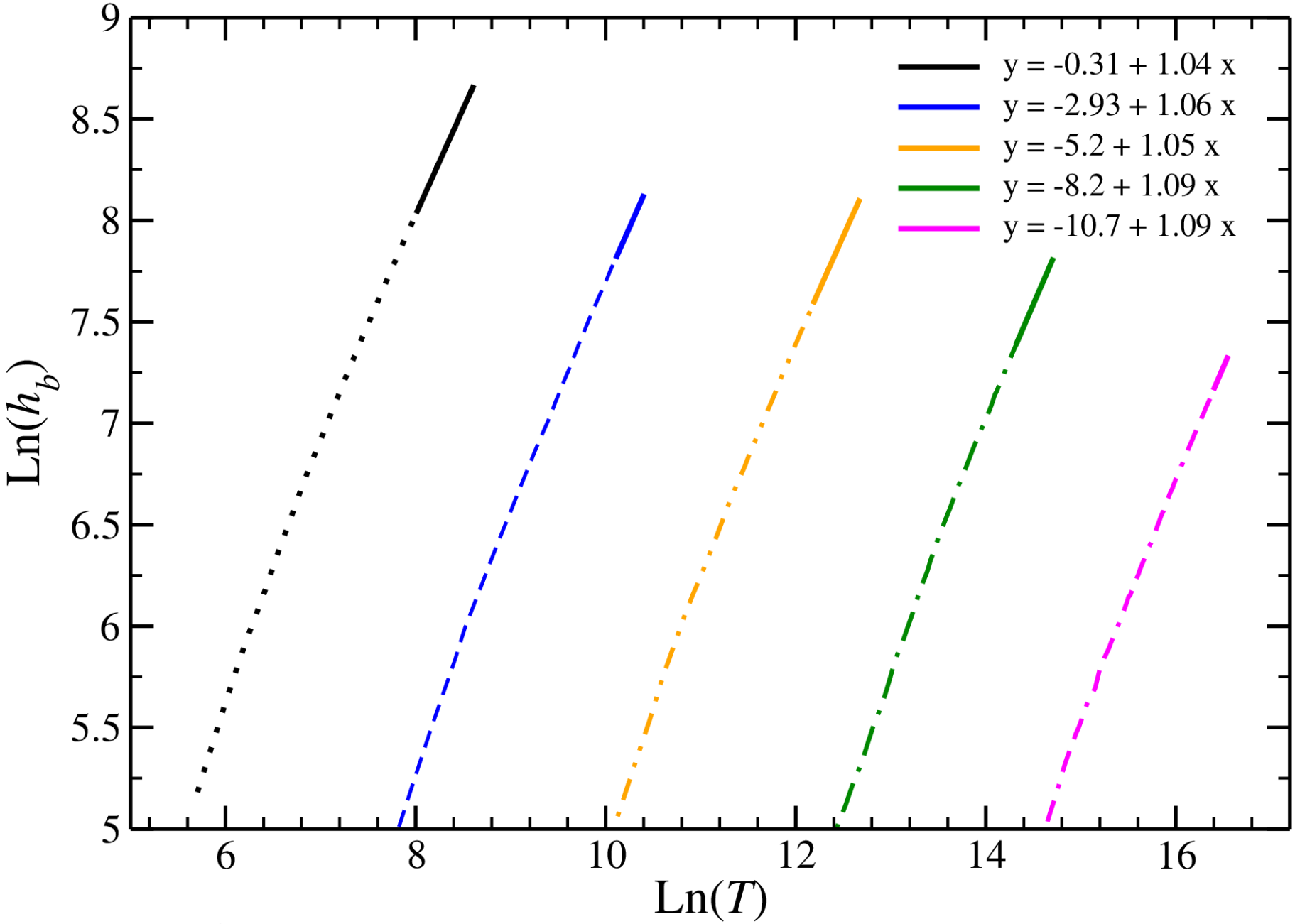
y = -0.31 + 1.04 x
y = -2.93 + 1.06 x
y = -5.2 + 1.05 x
y = -8.2 + 1.09 x
y = -10.7 + 1.09 x
Ln(h_b)
Ln(T)
9
8.5
8
7.5
7
6.5
6
5.5
5
6
8
10
12
14
16

figure 6

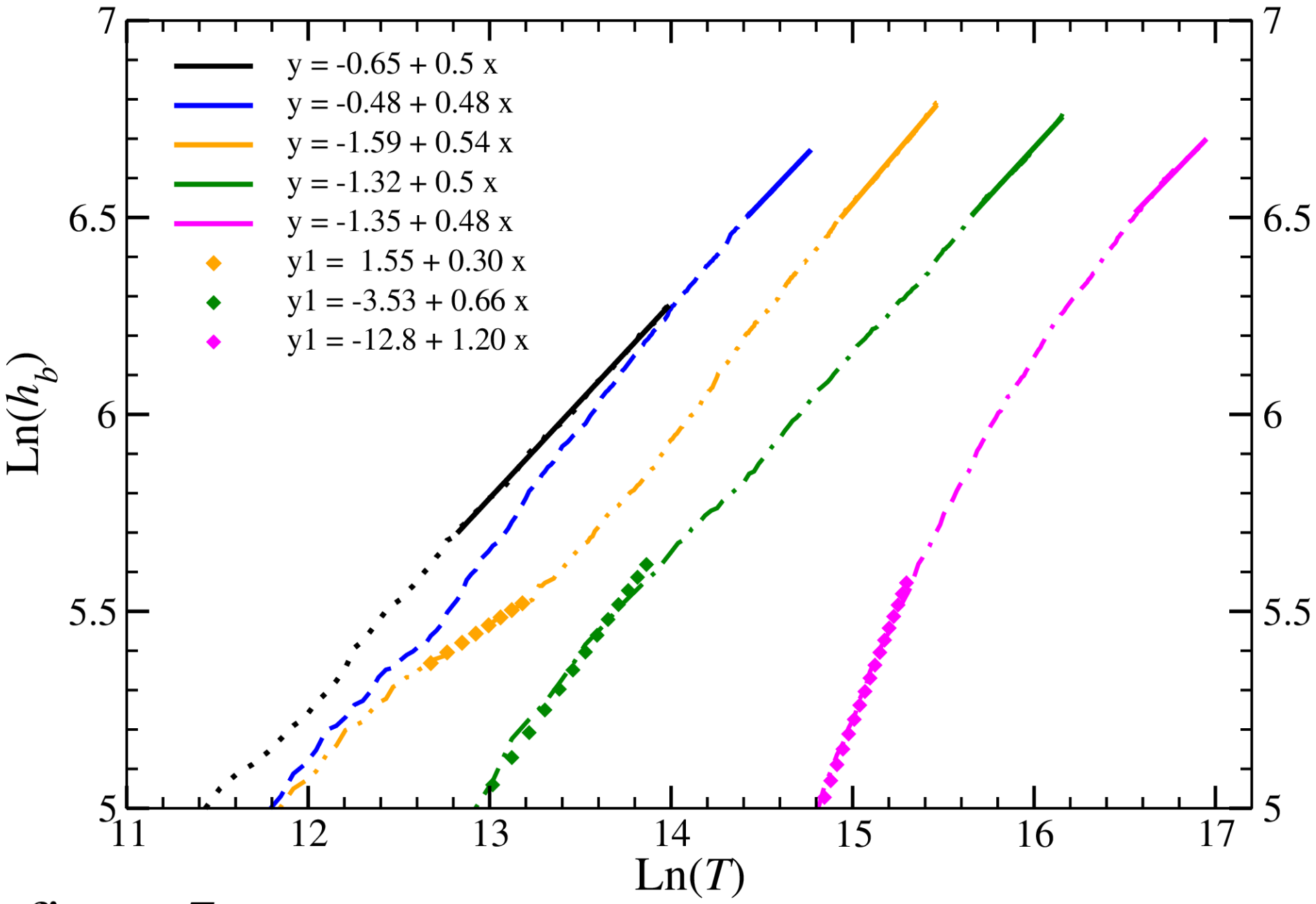
y = -0.65 + 0.5 x
y = -0.48 + 0.48 x
y = -1.59 + 0.54 x
y = -1.32 + 0.5 x
y = -1.35 + 0.48 x
y1 = 1.55 + 0.30 x
y1 = -3.53 + 0.66 x
y1 = -12.8 + 1.20 x
Ln(h_b)
Ln(T)
7
6.5
6
5.5
5
11
12
13
14
15
16
17

figure 7